scientific reports

OPEN

Design of planar distributed three beam electron gun with narrow beam separation for W band staggered double vane TWT

Cunjun Ruan✉, Pengpeng Wang, Huafeng Zhang, Yiyang Su, Jun Dai, Yikun Ding & Zheng Zhang

A novel planar distributed three-beam electron gun with narrow beam separations is designed based on grids loaded sheet beam method. The dimensions of the three-beam gun in the y–O-z plane are determined using our basic theoretical design method developed for sheet beam gun. The results show that the profile of focusing electrode in the y–O-z plane is related to the beam width in the x-O-z plane. Then, the characteristics and parameters of three-beam array formation with their stability are analyzed thoroughly by adjustment of control grids in the x-O-z plane. Each of the beamlet obtained is with a small axial deviation of the two transverse waists. Based on the theoretical analysis and simulations, the planar three-beam electron gun is constructed with the beam voltage of 22 kV and the current of 3 x 0.15 A. The average radius of 0.08 mm at each beam waist is obtained with the compression factor of 4 for the 0.18 mm beam tunnel radius. The beam waist can be achieved at about 4.4 mm away from the cathode with the axis separation about 0.46 mm for each of beamlet. Thus, the design method can be generally used to construct such type of narrow beam separation and planar distributed multiple beam electron gun for the miniaturization and integrated vacuum electron devices in millimeter wave and terahertz band.

High-power millimeter-wave and terahertz (THz) sources play a critical role in a wide spectrum of potential applications, including high-data-rate communications, biomedical diagnosis, chemical spectroscopy and threat detection[1–3]. Travelling wave tube (TWT) is a kind of vacuum electron devices (VEDs) which can provide high output power in a broad bandwidth[4]. However, the millimeter-wave or THz TWT combined with conventional circular beam is difficult to fulfill these demands due to the limitation of beam current carrying capacity. The adoption of a sheet beam can significantly promote the beam's current capacity, but the successive problems are difficulty in sheet beam focusing and an over-mode beam tunnel[5,6], which may also result in beam self-excitation and oscillation. However, planar distributed multi-beam TWT, with independent of beam tunnels and convergent beamlets, can achieve high output power by sustaining the total high beam current with a small current for each beam, which may avoid the over-mode beam tunnels comparing with the sheet beam devices. Moreover, the planar interaction circuit suitable for the planar distributed multi-beam array is not only easier in fabrication than the circular structures in the millimeter wave and THz regime, but also it can meet the trend of planarity, miniaturization and integration for next generation of vacuum electron devices[7,8].

Focused on the numerous advantages of integrated VEDs with planar multi-beam array, there is an increasing number of groups engaged in related research. The planar multi-beam arrays are not only used well in the folded waveguide TWT[9–12], but also used in the staggered double vane TWT[13,14]. Up to now, there are three kinds of planar multi-beam devices with unique interaction characteristics between the beamlets and the high-frequency field. Firstly, each beamlet matches an independent waveguide, which is identical to the single tube and operates in the fundamental mode. Thus, the adjacent axial separation in this kind of device is not limited and can be adjusted according to the level of fabrication. There are two typical works as following. In 2010, a 220 GHz three-beam cascaded serpentine TWT is developed[10]. The simulation using MAGIC-3D shows that the cascaded three-beam device can achieve a high-gain of 42 dB with a very compact circuit length of only 1.5 cm. As part of the DARPA HiFIVE program, Northrop Grumman Corporation developed a 220 GHz five-beam folded waveguide TWT in 2013 based on power combination among the five identical FWG circuit with finite gain[9]. The

School of Electronics and Information Engineering, Beihang University, Beijing 100191, China. ✉email: ruancunjun@buaa.edu.cn
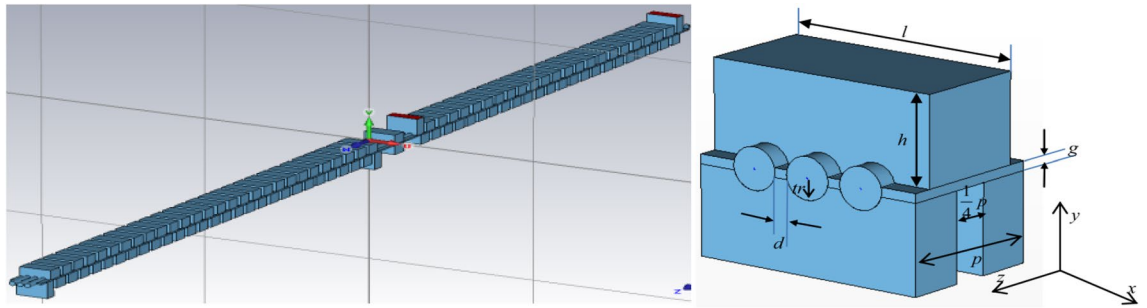
Figure 1. Schematic of W-band three-beam staggered double-vane TWT with the single period of the structure.

short pulse tests resulted in 56 W at 214 GHz and 5.0 GHz bandwidth. However, the spacing distance between the adjacent beam axes in both of the two devices is large enough to construct an independent electron gun for each beamlet. Thus, it is easy to obtain the well-converged beam array by a similar approach in multi-beam klystron[15]. Secondly, two or three beamlets may match a common interaction circuit using over-moded structure[11,14], e. g, the adjacent axial separation is about 1~2 mm for the over-moded multi-beam devices for W-band high power coherent radiation. Thirdly, two or three beamlets match a common interaction circuit, which operates in the fundamental mode[12,13]. The adjacent axial separation is, generally, less than 0.5 mm for 95 GHz and 0.2 mm for 220 GHz high output power tubes. Thus, for the latter two cases, it is challenging to develop new multi-beam gun design techniques to generate the desired planar multi-beam array with so narrow beam separation.

The present work in this paper is a part of our project study of "*W-band Multiple Beam High-power Staggered Double-vane TWT*"[13]. Since the designed staggered double-vane slow wave structure (SWS) operates in the fundamental mode (TM_{11}) under the first spatial harmonic, the spacing between adjacent beam axes is so narrow that is only 0.46 mm. To decrease the emission current density and keep the narrow beam separation, we'd like to construct a novel planar three-beam gun that combines the sheet beam gun with the special control grids[6].

In this paper, a novel planar distributed three-beam electron gun with narrow beam separations is theoretically designed based on grids loaded sheet beam method, which have been develop by our group recently[15]. This design method is a universal method which has been fully verified in reliability and stability to obtain planar electron beam by one-dimensional compression of cathode electron beam. Moreover, we have also analyzed and verified the stability of the designed electron gun, including the sensitive dependence on the geometric size, and some electric parameters such as voltage and current. Therefore, this novel design method can be widely used in millimeter wave and terahertz planar electron beam devices. Thus, compared with the relevant literature[15,16], a synthesized new method, which combines the theoretical analysis and numerical calculation is firstly adopted to design the novel planar three-beam gun with a narrow beam separation. Due to the plane symmetry of the three-beam array, the gun is designed the same as the profile of sheet beam gun with a whole throughout, which is different comparing with the conventional design concept of paraxial approximation for the structure construction with multiple beamlets[16,17]. Then, the dimensions and the position of the control grids are adjusted combined with the construction of a special focusing electrode to generate the desired planar three-beam array with the narrow beam separation. The good agreements have been achieved between the theoretical analysis and 3D simulation for the designed planar three-beam electron gun.

Design specifications and methodologies

The design W-band three beam high-power staggered double-vane (SDV) TWT with the scheme of a single period structure is given in Fig. 1, which shows the arrangement of the planar three electron beam with its SDV SWS. Thus, the design specifications of the planar three-beam electron gun are as follows. The operating voltage U_a and the beam current I are 22 kV and 3×0.15 A, respectively. Each of the beam tunnel radii is 0.18 mm and the axis separation of the adjacent electron beams is 0.46 mm. The three-beam array is characteristic with so narrow beam separation due to the space limitation in the x-axis of the fundamental mode, which will result in a high emission current density and a shrunk cathode lifetime based on conventional one circular beam electron gun. Thus, a novel planar distributed three-beam gun based on grids loaded sheet beam gun is developed, and the guidelines of design methodologies are presented in the paper.

Figure 2 shows the schematic of the three-beam gun in both two transverse directions. It's obvious that the outline of the three-beam gun is constructed identically to the sheet beam gun with the same profile except for the focusing electrode. In the following discussion, the centers of three beamlets are at x = -0.46 mm, y = 0 mm, at x = 0, y = 0, and at x = 0.46 mm, y = 0, respectively. Three-beam array emits electrons from the cathode that locates at z = 0, which will be transported along the positive direction of the z-axis.

Figure 3 shows the logical diagram that indicates the detailed design guidelines of the novel planar three-beam gun with narrow beam separation in this paper. Apparently, the design process of the planar three-beam gun can be simply divided into two steps. Firstly, the dimension of the three-beam gun in the y–O-z plane is determined based on the theory guideline for designing Pierce-type sheet beam gun as our work in reference[15]. In this step, several key parameters of the three-beam gun can be determined, including the half-angle θ, curvature radius of cathode R_c and anode R_a, spacing from cathode to anode dK_a, half-height of anode aperture r_a. Then the simulations are used to verify the key parameters and beam transport in y–O-z plane thoroughly. Secondly,
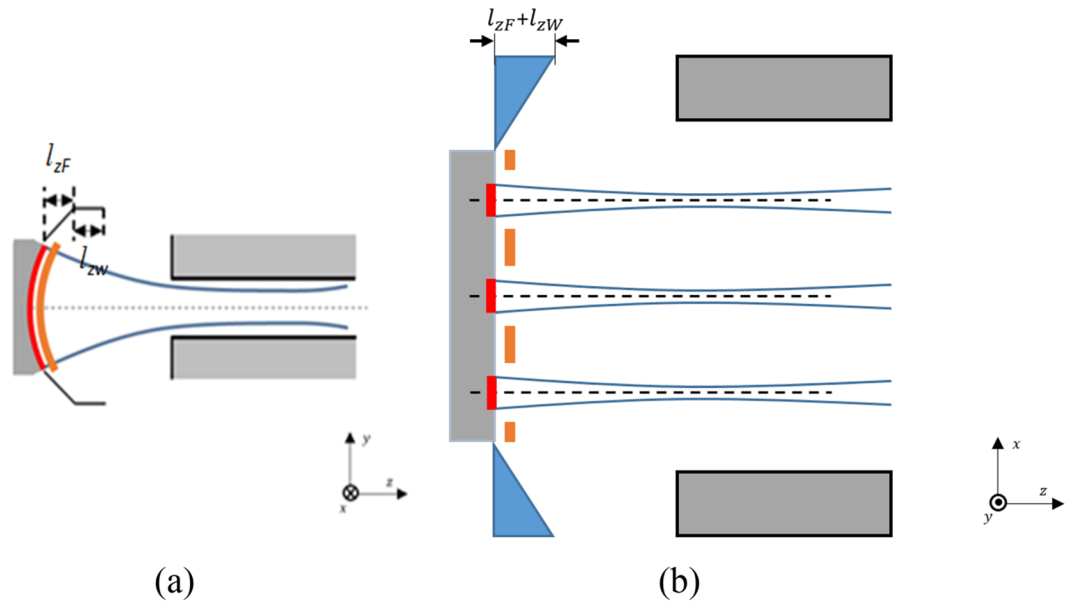
Figure 2. Schematic of the novel planar three-beam electron gun in both two transverse directions. (**a**) Front view. (**b**) Top view.
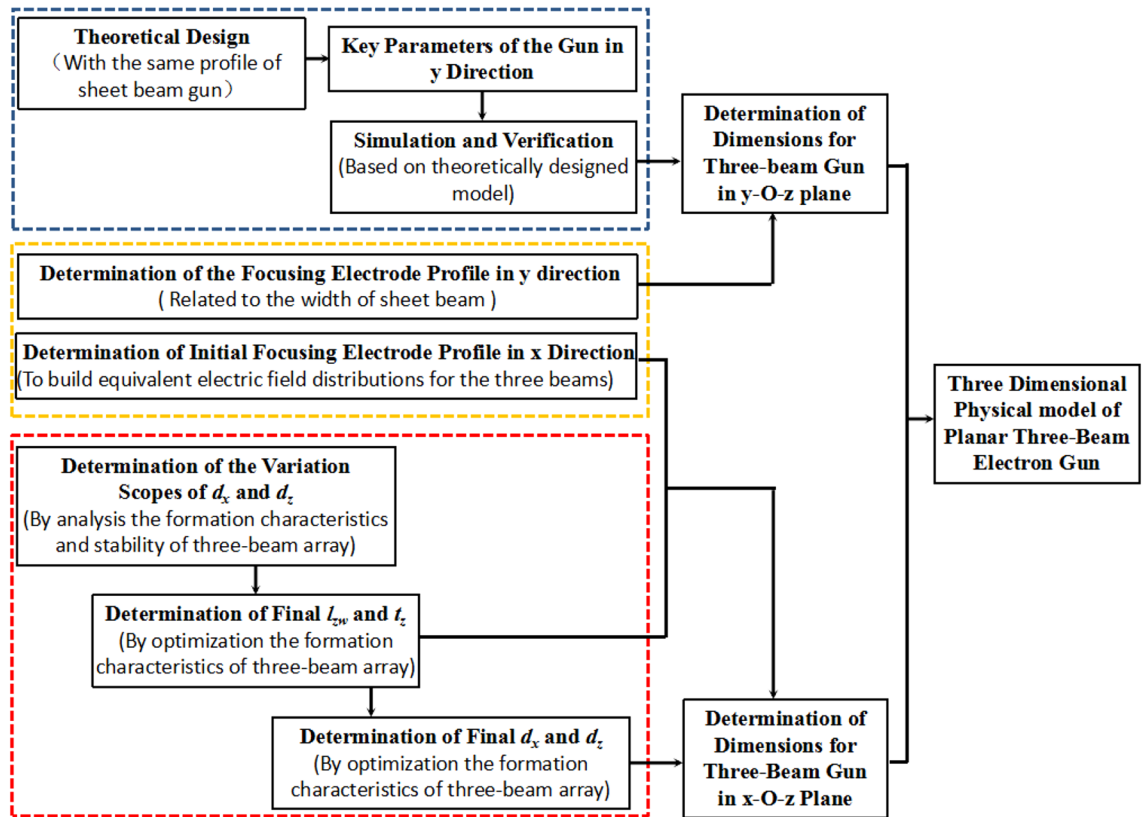
Figure 3. Logical diagram of the design guidelines for the novel planar three-beam electron gun.

the dimension of the three-beam gun in the x-O-z plane is determined based on the scopes analysis for the formation characteristics and stability of three-beam array with several parameters optimization, which includes the separation between adjacent grids wires d_x, the extension length of focusing electrode l_{zW}, the thickness of the control grids t_z, and the separation from cathode to grid d_z focusing electrode. The results show that the determination of the profile of focusing electrode in two directions can be included in the two steps, respectively.
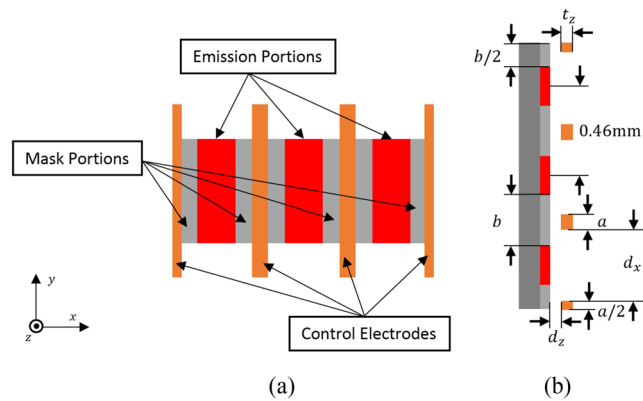
Figure 4. Configuration of the three-beam cathode combined with the control grids. (**a**) Right view. (**b**) Top view.

Figure 4 shows the configuration of the three-beam cathode combined with the control grids. Width (dimensions in x direction) of the side portions of the control electrodes ($a/2$) and the masks ($b/2$) equal half of their counterparts, respectively, which is located in the middle of the structure to construct the equivalent electric field distributions for the side beams and the central beam. To obtain the excellent beam transmission of the three-beam array, we'd like to keep a smaller beam-to-tunnel radial fill factor. The intended average radius at the beam waist is about 0.08 mm. Thus, half-height of the emission portion is about 0.32 mm with the selected beam compression factor of 4 in y direction. Half-width of each emission portion is chosen as 0.1 mm with compromising the lower emission current density and the focusing characteristics of the control grids. Finally, the cross-sections of each emission portion and the complete cathode are about 0.2 mm × 0.64 mm, and 1.38 mm × 0.64 mm, respectively. The compression factor of each beamlet in y direction is set to 4, which means that the current emission density of 117 A/cm^2 is required for the cathode. Such high emission density can be satisfied with a new type of impregnated dispenser cathode using the active substance with a molar ratio of 26BaO·29SrO·8Sc$_2$O$_3$·7CaO·Al$_2$O$_3$, which can achieve the electron beam emission density of over 160 A/cm^2 experimentally in reference[18].

In part III of this paper, we show that the dimension of the three-beam gun in the y–O-z plane is determined based on the theory guideline for designing Pierce-type sheet beam gun as our work in reference[17]. Each electron beam formation comes from a narrow rectangle cathode, which is only compressed in y direction with a ratio of 4. However, in part IV, we constructed the desired electric field distribution by the focusing electrode combined with the control grids, which is different from conventional Pierce-type guns, attaining the same proper beam size in the x direction. As a result, the rectangle electron beam in the beam waist is formed with the same dimension in x and y direction. Thus, in our manuscript, we use the description of radium symbols, e.g., the R and r which are widely used in the design of the traditional round electron beam. Such a description only denotes that our designed three electron beams have the same dimension in x and y direction.

Dimensions of the three-beam gun in y–O-z plane

In this section, several key dimensions of the three-beam gun in the y–O-z plane are determined based on the extended theoretical method used for designing sheet beam gun with the same profile in reference[17]. Simulation results show that the required length l_{zW} of the focusing electrode and the beam throw distance z_m are different according to the beam width in x direction. Thus, an appropriate range of l_{zW} and z_m will be estimated appropriately for the design of the three-beam gun.

Figure 5 shows some important parameters for the design of sheet beam electron gun[17] in this paper. Here we emphasize that R_c and R_a are the curvature radius of the cathode and the anode. θ is the half-angle, which means the angle between the cathode edge and the convergence point when the sheet beam passing through the anode aperture. θ' is the new half-angle under the influence of the divergence of the anode aperture. θ'' is the equivalent half-angle considering both the convergence of the initial sheet beam and the divergence of the anode aperture. r_c is the half height of the cathode while r_a is the half height of the anode aperture. It's obvious that θ only depends on R_a (or R_c) when R_c/R_a is given.

Determination of half-angle θ.
According to the designed three-beam gun model, the current of beam portion with unit width I_u can be calculated as 0.75 A/mm according to reference[17]. The design curves of beam compression factor and throw distance for the sheet beam gun are shown in Fig. 6, respectively. According to Fig. 6(a) with the beam compression factor of 4, the value of the curvature radius ratio of the cathode to anode R_c/R_a can be calculated as 2.464. Next, the L-B function $(-\beta_a)^2$ can be consulted from the chart of $(-\beta)^2 \sim R_c/R$ [Table III in[19]] as 1.705. Then, substituting the value of $I_u, U_a, (-\beta_a)^2$ into
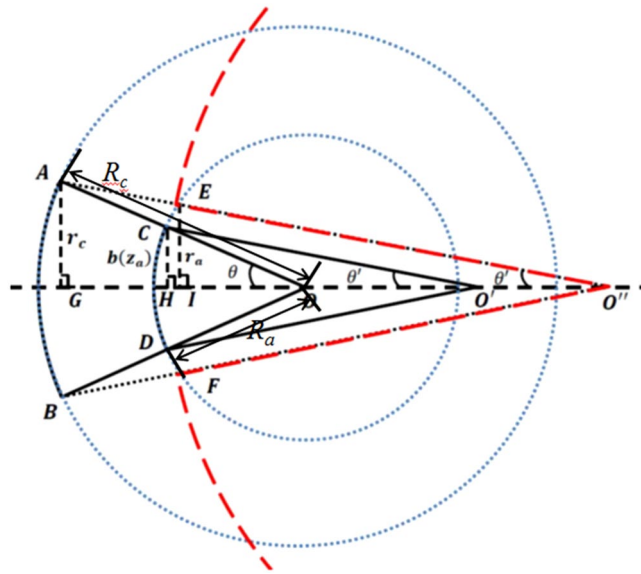
Figure 5. Schematic of the sheet beam electron gun with their parameters.
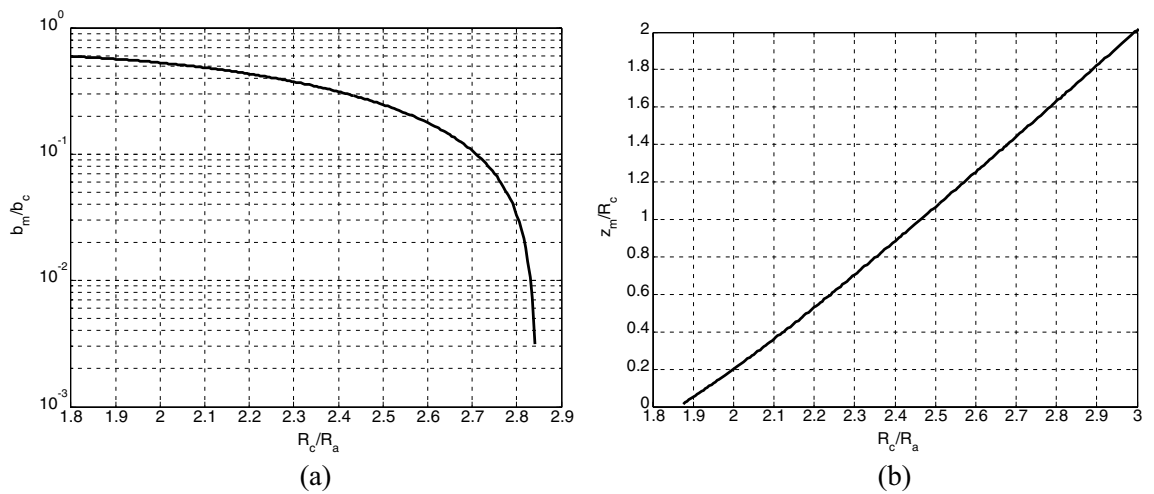
Figure 6. Design curves of sheet beam gun for (**a**) compression factor and (**b**) throw distance.

$$I_u = 14.67 \times 10^{-6} \frac{\theta}{\pi} \frac{U_a^{3/2}}{R_a(-\beta_a)^2} \tag{1}$$

the curvature radius of anode R_a can be expressed in θ

$$R_a = 11.924\theta \tag{2}$$

The curvature radius of cathode R_c can be expressed as

$$R_c \approx \frac{b_c}{\theta} \tag{3}$$

Combining (2) and (3) with considering the value of R_c/R_a, the half angle θ can be calculated as 5.983 degrees.

Determination of other parameters for sheet beam gun. According to the following formulas (4), (5), (6), the value of R_c, R_a, and the spacing from cathode to anode dK_a can be calculated as 3.070 mm, 1.246 mm, 1.814 mm, respectively.

$$R_c = \frac{b_c}{\sin\theta} \tag{4}$$
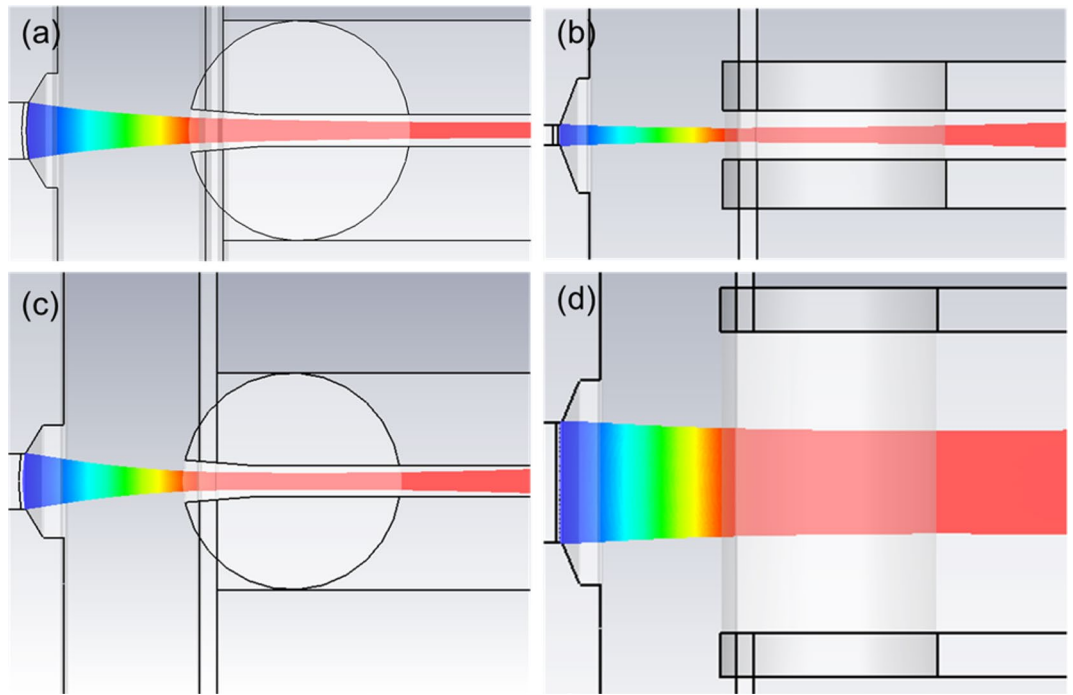
Figure 7. Beam trajectory in two transverse directions for the two models. (**a**) In the y–O-z plane of Model I. (**b**) In the x-O-z plane of Model I. (**c**) In the y–O-z plane of Model II. (**d**) In the x-O-z plane of Model II.

$$R_a = \frac{R_c}{R_c/R_a} \tag{5}$$

$$dK_a = (R_c - R_a) \cdot \cos\theta \tag{6}$$

The throw distance z_m can be obtained as 3.011 mm from Fig. 6(b) with the value of R_c/R_a.

According to the advanced method for anode aperture reconstruction in sheet beam gun, half-height of the reconstructed anode aperture r_a can be calculated as 0.245 mm. Considering the correction of cylindrical aberration, the key parameters for sheet beam gun can be determined successfully.

Simulation and verification.

To verify the effectiveness of the theoretical method above for design sheet beam guns and study the characteristics of a focusing electrode, two sheet beam gun models with different cathode cross-sections are constructed using CST PS model[20,21], which are of single emission portion (Model I) and the complete cathode (Model II) of the three-beam gun, respectively.

A focusing electrode in sheet beam gun is constructed with the electric field distribution for wedge-shaped converging radial flow. In our sheet beam gun model, the focusing electrode profile in the y direction is preliminary composed of two tiled metal walls which makes an angle of 67.5^0 with the normal to the cathode followed by two parallel metal planes. Combined with 3D simulation software CST PS, the proper axial dimensions of the tiled parts in the two models are both $l_{zF} = 0.2$mm, but of the parallel portions are $l_{zW} = 0.13$mm for Model I and $l_{zW} = 0.24$mm for Model II, respectively, when both of them are performed well.

Simulated beam trajectories of the two models are shown in Fig. 7. Figure 8 compares the simulated beam envelops in the y direction of the two models. Apparently, both of the two sheet beams achieve their intended waist of 0.08 mm. However, the throw distances z_m in the two models are quite different. A further throw distance, 5.5 mm, is more likely to take place in Model I (with a smaller beam width). However, the throw distance in Model II is about 3.5 mm.

The main reason for the differences above in l_{zW} and z_m in two models may be that the y components of spacing charge force in sheet beams are different with various beam width in x direction, which results from the influence of beam boundary distortion. A smaller y component for the space charge force is with the smaller width sheet beam due to a more serious influence of boundary distortion in it. Thus, the convergent effect of the focusing electrode needed in Model I should be less than it needed in Model II. Consequently, an intermediate convergent effect of the focusing electrode is needed in our three-beam gun, 0.13 mm $< l_{zW} <$ 0.24 mm. And the throw distance of each beamlet in our three-beam array may be more than 3.5 mm and less than 5.5 mm.

From the calculation, the beam current is about 0.155 A for Model I and 1.076 A for Model II corresponds to the unit beam current of 0.78 A/mm, which is close to the expected value 0.75 A/mm. Thus, the effectiveness of the above method for designing a sheet beam gun is verified and the key parameters will be used in the following three-beam gun construction.
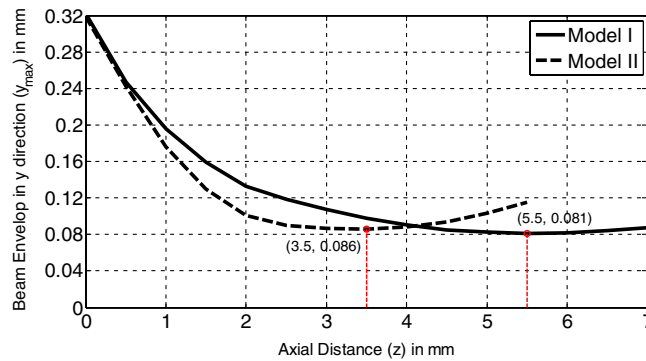
**Figure 8.** Compressions of beam envelops in *y* direction of the two models.
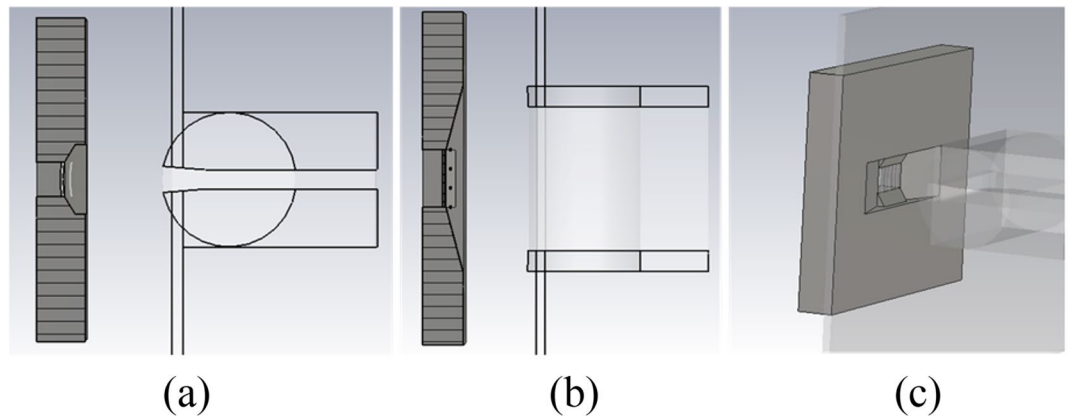
Figure 9. Configuration of the focusing electrode in the three-beam electron gun. (**a**) In the y–O-z plane. (**b**) In the x-O-z plane. (**c**) 3D view.

Determination of the dimensions for three-beam gun in x-O-z plane with beam formation stability

Based on the analysis, the overall outline of the novel three-beam gun in the x-O-z plane can be initially built according to the sheet beam gun in Model II. However, the focusing electrode profile should be unique for the three-beam gun with the reason of different electric field distributions required for beam compression of the three-beam array and the sheet beam. In the novel three-beam gun, the desired electric field distribution for three convergent beamlets is constructed by the focusing electrode combined with the control grids. Their characteristics decide the performance of the three-beam gun directly and effectively. In our model, the potentials of the focusing electrode and the control grids are set at the cathode potential to make the simplicity and stable operation of the gun. In this section, the profiles of focusing electrode in two transverse directions are determined, respectively, for the equivalence of three beamlets with good beam characteristics. Transmission verification of the beamlet with transverse velocity in the axial Brillouin magnetic field is carried out theoretically. At last, several key dimensions of the control grids are discussed based on the characteristic's analysis of the three-beam array formation.

Focusing electrode profile in x direction. Non-equivalence of the beamlets with different lateral positions in the three-beam array may cause quite a few problems in the following transport process under the magnetic field by the focusing structure. To generate three beamlets with similar properties, a novel focusing electrode is constructed in the paper, which can adjust the electrical field distribution in two transverse directions independently.

Figure 9 shows the configuration of the novel focusing electrode structure for the three-beam gun. The focusing structure profile in y direction is identical to the configuration in the sheet beam gun above. However, the profile in the x direction is without the two parallel metal plane parts, and the inclination angle of the focusing electrode in x direction called θ_{FX} is larger. By the much more numerical simulation analysis on various three-beam gun models, the beam current of each beamlet reaches an approximately identical value when θ_{FX} increase to a constant value. It's about 1.13 times of 67.5^0, e.g. the center point is 76.275^0, which can make the three beamlets transport along their symmetric axes strictly. However, the side beam currents are less than the value of central one and the side beamlets are all tilting towards the gun center with beam transport, when θ' is less than
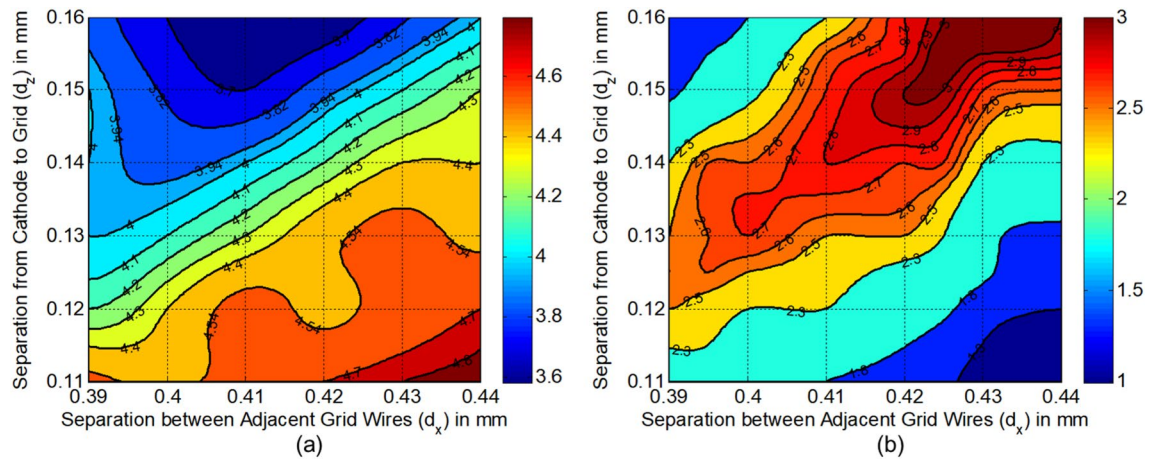
Figure 10. (**a**) Variation of throw distance in y direction Z_{mY} with both d_x and d_z. (**b**) Variation of throw distance in x direction Z_{mX} with both d_x and d_z.

the critical point. This may be caused by a more convergent electric field distribution constructed by the focusing electrode in the x direction, which also constrains the electrons emission from the side emission surfaces.

Determination of the variation scopes of d_x and d_z. The preliminary determinations of the variation scopes of transverse dimensions d_x and axial position d_z of the control grids will facilitate the determinations of the other parameters and the design work of the novel three-beam gun, in Fig. 2. Thus, the variations of the two parameters are primarily discussed based on their effects on the throw distances in both two transverse directions.
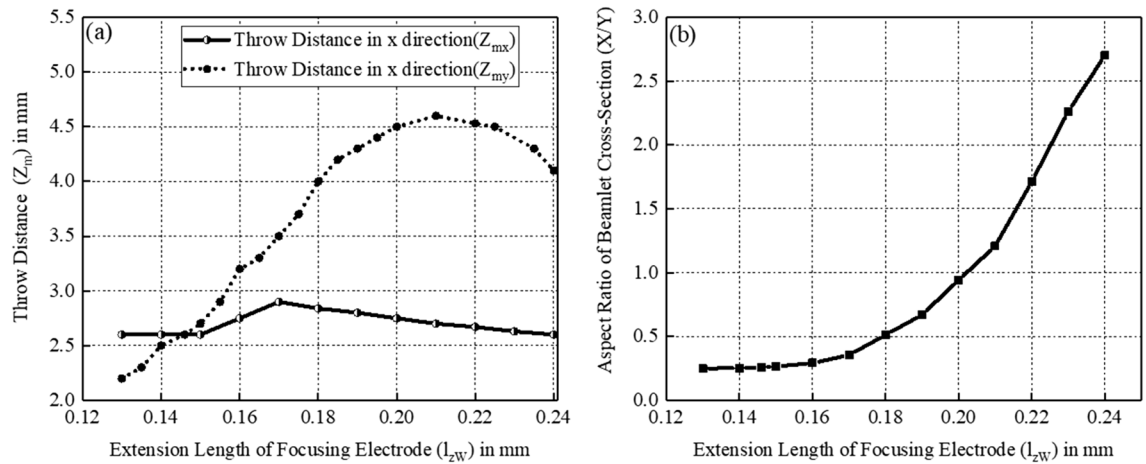
Figure 10(a) gives the variation of throw distance in the y direction Z_{mY} with both d_x and d_z. In our calculation, we have selected the calculation points for d_x from 0.39 to 0.44 mm, and d_z from 0.11 to 0.16 mm with the small intervals of 0.002 mm, so that there are much of enough original data which can express the characteristics and tendency in all the similar figures in our paper. Also, we have used cubic spline interpolation in plotting all the figures with MATLAB to achieve good smoothness for all the curves in these figures. From the results, it's clear that Z_{mY} almost remains constant while keeping the variation ratio of d_x and d_z unchanged. And the linear change range of Z_{mY} is mainly from 4.0 to 4.4 mm. Besides, the results verify the deduction in the following subsection that throw distance of each beamlet for three-beam may be more than 3.5 mm and less than 5.5 mm.

Figure 10(b) gives the variation of throw distance in the x direction Z_{mX} with both d_x and d_z. The models with $Z_{mX} < 2.3$ in the top left corner are invalid due to the trajectories cross each other under the stronger convergent function in the x direction. With considering the calculated spacing from cathode to anode $dK_a = 1.814$ mm, the models with $Z_{mX} < 1.8$ in the bottom right corner are invalid due to the beam waist in the x direction hasn't emerged into anode aperture. Thus, the upper limit of d_x and d_z are selected at 0.44 mm and 0.16 mm, respectively, to keep a wider valid range of data. Besides, Z_{mX} is shrunk dramatically with minimizing d_z and d_x simultaneously at a constant ratio of d_x and d_z, but Z_{mY} almost keeps constant according to Fig. 10(a). To facilitate the design work and matching process of the magnetic focusing system, the three-beam gun with smaller waists separations among the two transverse directions are desired. Thus, the lower limits of d_x and d_z should not be too small. Consequently, the proper region of d_x and d_z are determined as to 0.39 mm ~ 0.44 mm and 0.11 mm ~ 0.16 mm, respectively.

Determination of extension length of focusing electrode l_{zW} and t_z. Throughout the analysis on focusing electrode above, all dimensions of the focusing electrode in the novel three-beam electron gun are determined except the parameter l_{zW}, which will be discussed in this subsection combined with the consideration of beam transport characteristics on both x and y directions. Control grids that serve as the 'focusing electrode' in the x direction control the formation and transport of the beamlets in x direction. The thickness of the control grids t_z is also selected in this subsection based on the beam transport characteristics analysis for both transverse directions.

From the above analysis, the three-beam gun model with intermediate values of $d_x = 0.415$ mm and $d_z = 0.13$ mm is selected to study the axial characteristics of focusing electrode and control grids, including l_{zW} and t_z. Figure 11(a) shows the variation of throw distances in both x and y directions with l_{zW}. Figure 11(b) shows the variation of the aspect ratio (X/Y) of beam cross section at beam waist in y direction with l_{zW}. According to Fig. 11(a), the throw distances in both transverse directions meet in the gun model with $l_{zW} = 0.146$ mm. However, according to Fig. 11(b), the aspect ratio of beam cross-section in this model is about 0.257 that close to the aspect ratio of cathode 0.313 and is far from the desired circular beam. According to Fig. 11(a), it's obvious that the throw distance in y direction Z_{my} is raising with the extended length l_{zW} of focusing electrode since the incidence slope of boundary electrons are increased. The reason for the drop of Z_{my} at $l_{zW} = 0.24$ mm is that electron trajectories from different layers cross each other. However, the throw distance in y direction Z_{mx} is relatively insensitive to l_{zW}. To facilitate the design work of the following magnetic focusing system, the beam

Figure 11. (**a**) Variation of throw distances in both *x* and *y* directions with l_{zW}. (**b**) Variation of aspect ratio of beam cross section at beam waist in *y* direction with l_{zW}.
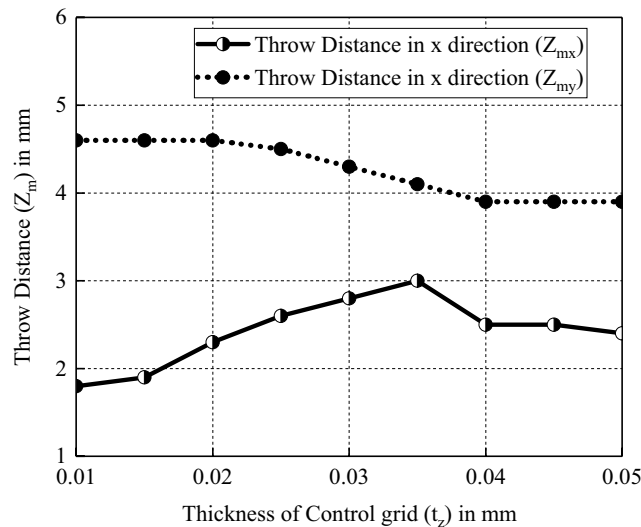

Figure 12. Variation of throw distances in both *x* and *y* directions with t_z.

array with a closer beam waist in both transverse direction is desired, which means a shorter l_{zW} according to Fig. 11(a). Besides, the value of l_{zW} should not be too small from Fig. 11(b) to make the cross-section at the beam waist close to be circular. Thus, the value of l_{zW} is compromised as 0.19 mm with the aspect ratio of beam cross-section at the waist about 0.7.

After determining the value of l_{zW}, we explored the influence of the value of t_z on the throw distances in both *x* and *y* directions, as shown in Fig. 12. It's obvious that the throw distance in the x direction Z_{mx} is increasing with t_z firstly and begins to drop beyond the critical point of $t_z = 0.035$ mm. But the throw distance in the y direction Z_{my} always decreases as t_z increases. Thus, a greater thickness of control grids but no more than 0.035 mm would be like for a narrower axial separation between two beam waists. Considering the stability of the gun and the machining error, $t_z = 0.03$ mm is selected as the thickness of the control grid.

Determination of d_z and d_x with beam formation stability. Based on the structure of the three-beam gun determined, the value of d_x and d_z are in the scope of 0.39 mm ～ 0.44 mm and 0.11 mm ～ 0.16 mm, respectively. In this range, Fig. 13(a) shows the variation of beam current and stability with d_z and d_x. It's found that the beam current is decreasing with enhancing d_z, or minimizing d_x, and the beam current almost unchanged and kept more stability with broadening d_z and d_x simultaneously. According to the design specification, the values of d_z and d_x that keeps the beam current varies in the range of 0.145 A ～ 0.155 A could be selected easily.

Figure 13(b) shows the variation of beam aspect ratio (x/y) at the beam waist in the y direction with d_z and d_x. It can be seen that the aspect ratio mainly increases with minimizing d_z, or enhancing d_x in the scope where the beam current is acceptable. Considering the stable beam transport in the following magnetic field, the beam aspect ratio is better limited from 0.67 to 1.
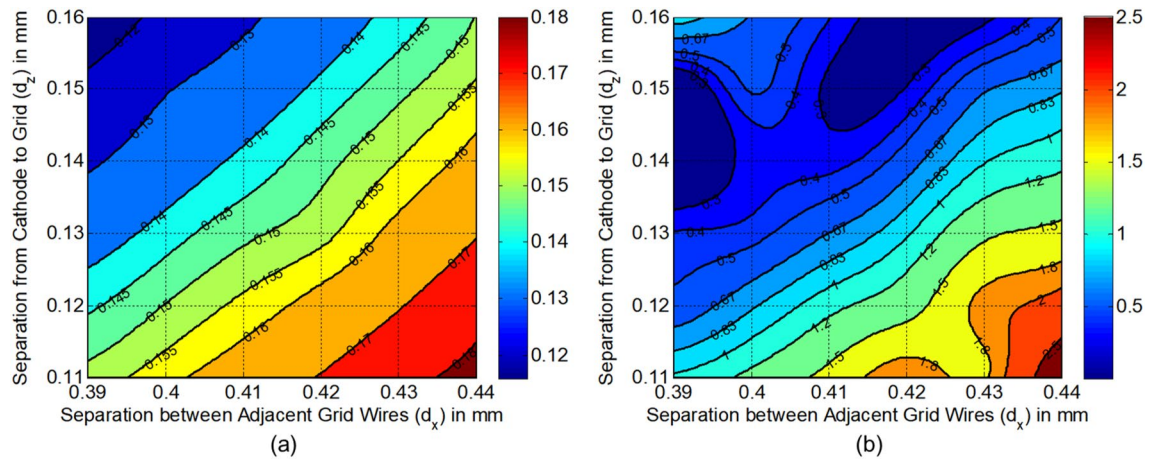
Figure 13. (**a**) Variation of beam current with d_z and d_x. (**b**) Variation of beam aspect ratio (x/y) at the beam waist in y direction with d_z and d_x.
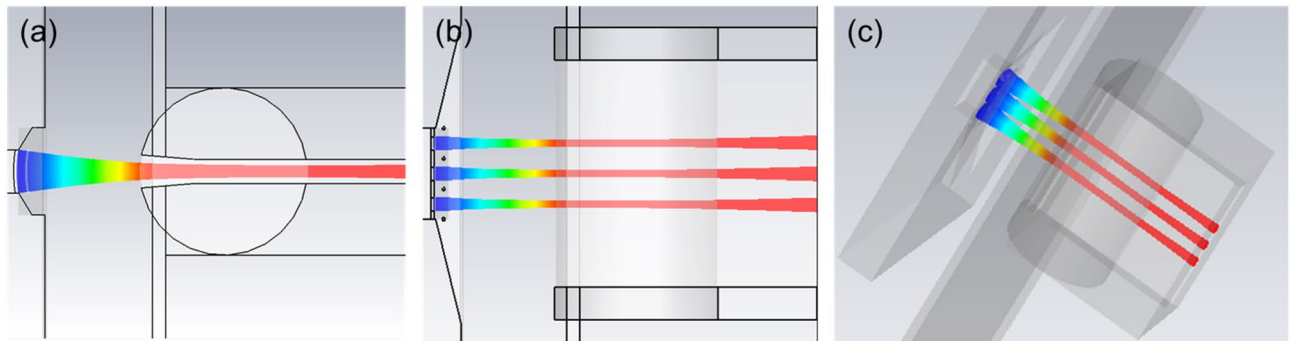
Figure 14. Beam trajectory of the novel planar three-beam gun. (**a**) In the y–O-z plane. (**b**) In the x-O-z plane. (**c**) 3D view.

When the proper combinations of d_z and d_x are selected, Fig. 11(a) and (b) should be taken into consideration to verify if the model is with a small waist separation in the two transverse directions.

Construction and simulation. To guarantee the good beam characteristics and satisfy the demands from the high frequency circuit, the three-beam array with the beam waist aspect ratio from 0.67 to 1 and the beam current from 0.145 A to 0.155 A would like to be taken into consideration. The combination of $d_z = 0.13$ mm and $d_x = 0.415$ mm is finally adopted in our design for the novel planar three-beam electron gun with CST simulation[20,21]. Figure 14 shows the three-beam array is well generated and compressed on both two transverse directions. Figure 15 shows the beam cross-section along the direction of beam transport. The three-beam array achieves the waist in the x direction at about 2.5 mm away from the cathode, and achieves the waist in y direction at about 4.4 mm away from the cathode. The profiles at beam waists in the x direction and the y direction are indicated in (c) and (e), respectively. The beam aspect ratio at the waist in y direction is about 0.83. And the simulated beam current is about 3×0.153 A.

For the design of our three-beam electron gun with small distances between cathode, focusing electrode and anode, the high voltage will cause the breakdown due to the strong electric field strength. As we know, with the high vacuum ($\sim 10^{-7}$ Pa–10^{-8} Pa), the breakdown field strength is more than 10^6 V/cm as the experienced data. However, from the electric field distribution in our designed three-beam electron gun with CST PS, we know the maximum electric field of the whole structure is about 3×10^5 V/cm (the maximum electric field appears in the four corners of the edge the focusing electrode), which is smaller than the breakdown electric field of 10^6 V/cm in high vacuum. Thus, the breakdown in our electron gun cannot happen.

Conclusion

Only by developing in the direction of planarization, miniaturization and integration, can the vacuum electronic devices be expected to break through the limitations of existing mechanisms, and thus achieve leapfrog development in the THz band. In this paper, methodologies and guidelines for designing the novel planar distributed three-beam electron gun are presented with narrow beam separations, which can be used in such type of narrow separation beam electron gun as one of the general method. The physical model of our novel planar three-beam gun with optimal characteristics is verified using simulation in the 3D software, the beam current of 3×0.15 A,
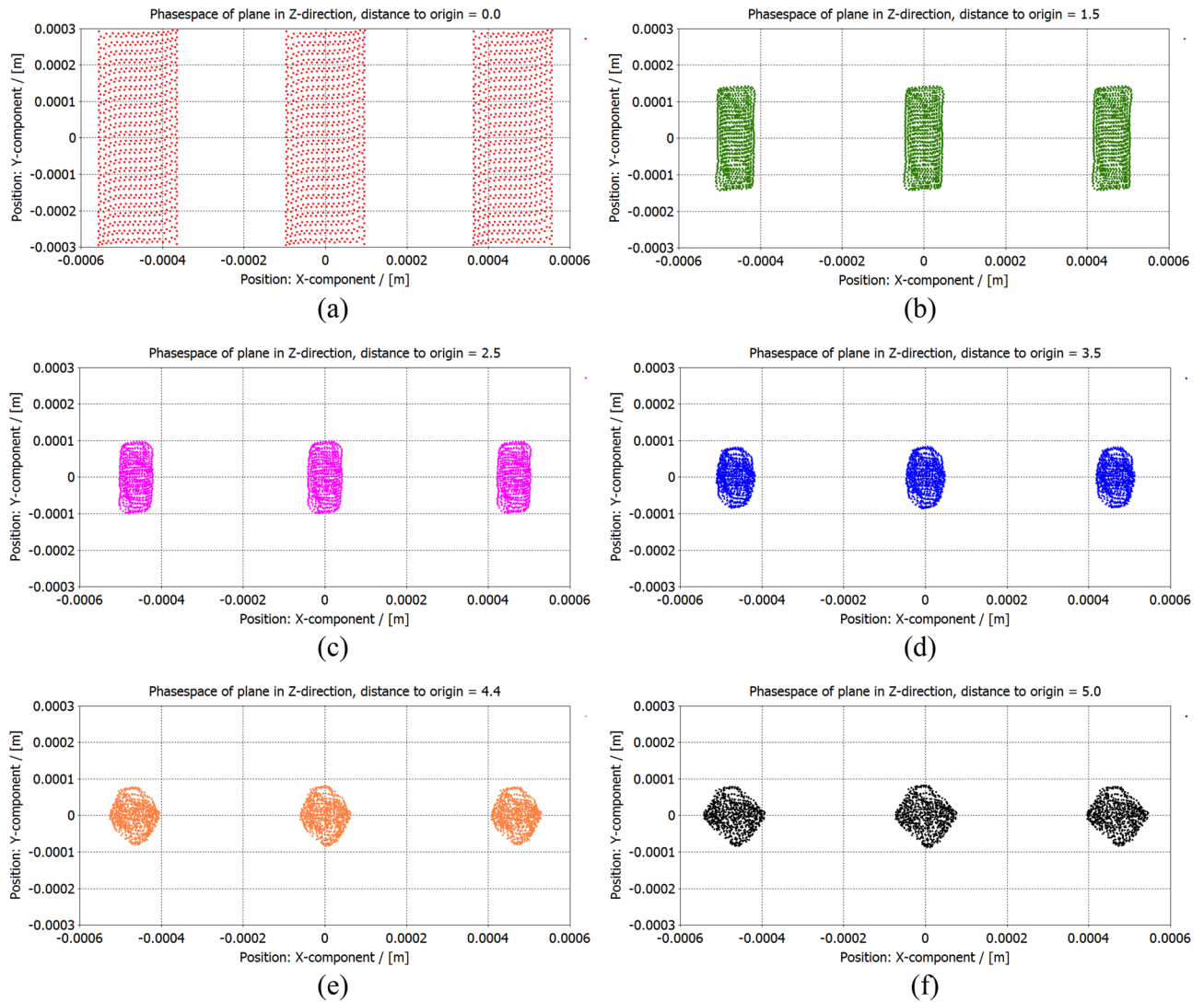
Figure 15. Beam cross-section along the direction of beam transport. (**a**) z = 0, (**b**) z = 1.5 mm, (**c**) z = 2.5 mm, (**d**) z = 3.5 mm, (**e**) z = 4.4 mm, (**f**) z = 5.0 mm.

an average beam radius of 0.08 mm for each beamlet waist is obtained successfully with a beam compression ratio of 4. Consequently, the designed three-beam electron gun will be used in our fundamental mode staggered double vane TWT in W-band with high output power later. Moreover, such planar distributed multi-beam with independent beam tunnels and singly convergent beamlets, can achieve high output power by sustaining the high total beam current, and avoids the over-mode beam tunnels comparing with the sheet beam devices. Such novel scheme for the planar multiple beam combined with the planar interaction circuit are not only suitable for the planar distributed vacuum electron devices, e.g. traveling wave tube, extended interaction klystron and oscillator, in widely range for the millimeter wave and THz regime, but also it can meet the trend of planarity, miniaturization and integration for the development of next generation of vacuum electron devices with good potential for the high output power and broad bandwidth in the future.

References

1. Parker, R. K., Abrams, R. H., Danly, B. G. & Levush, B. Vacuum electronics. *IEEE Trans. Microw. Theory Tech.* **3**, 835–845 (2002).
2. Korolev, A. N. *et al*. Traditional and novel vacuum electron devices. *IEEE Trans. Electron Devices* **12**, 2929–2937 (2001).
3. Booske, J. H. Plasma physics and related challenges of millimeter-wave-to-terahertz and high power microwave generation. *Phys. Plasmas* **15**, 459–597 (2008).
4. Siegel, P. H. Terahertz technology. *IEEE Trans. Microwave Theory Tech.* **50**, 910–928 (2002).
5. Han, Y. & Ruan, C. J. Investigation of the diocotron instability of an infinitely wide sheet electron beam by using the macroscopic cold-fluid model theory. *Chin. Phys. B* **10**, 104101 (2011).
6. Galdetskiy, A. V. On the opportunity of bandwidth increasing in multibeam klystron with planar layout of the beams. 12ᵗʰ IEEE International Vacuum Electronics Conference, Bangalore, India, doi:https://doi.org/10.1109/IVEC.2011.5747003. 21–24 Feb (2011).
7. Kong, L. *et al*. Enhancing spoof surface-plasmons with gradient metasurfaces. *Sci. Rep.* **5**, 8772 (2015).

8. Liu, W. *et al.* Design of uniform permanent magnet electronic optical system for 220 GHz sheet electron beam traveling wave tube. *Sci. Rep.* **10**, 13680 (2020).
9. Kreischer, K. E., Tucek, J. C., Basten, M. A., & Gallagher, D. A. 220 GHz power amplifier testing at Northrop Grumman. 14th IEEE International Vacuum Electronics Conference, Paris, France, doi:https://doi.org/10.1109/IVEC.2013.6570961. 21–23 May (2013).
10. Nguyen, K. *et al.* Design of a high-gain wideband high-power 220-GHz multiple-beam serpentine TWT. 11th IEEE International Vacuum Electronics Conference, Monterey, USA, doi:https://doi.org/10.1109/IVELEC.2010.5503621. 18–20 May (2010).
11. Gong, Y. *et al.* A 140-GHz two-beam overmoded folded-waveguide traveling-wave tube. *IEEE Trans. Plasma Sci.* **3**, 847–851 (2011).
12. Yan, S., Su, W., Wang, Y. & Xu, A. Design and theoretical analysis of multibeam folded waveguide traveling-wave tube for Subterahertz radiation. *IEEE Trans. Plasma Sci.* **1**, 414–421 (2015).
13. Ruan, C. *et al.* W-band multiple beam staggered double-vane traveling wave tube with broad band and high output power. *IEEE Trans. Plasma Sci.* **7**, 2132–2139 (2015).
14. Gee, A. & Shin, Y. M. Gain analysis of higher-order-mode amplification in a dielectric-implanted multi-beam traveling wave structure. *Phys. Plasmas* **7**, 073106 (2013).
15. Liang, H., Ruan, C., Xue, Q. & Feng, J. An Extended Theoretical Method Used for Design of Sheet Beam Electron Gun. *IEEE Trans. Electron Devices* **11**, 4484–4492 (2016).
16. Nguyen, K. T. *et al.* Electron gun design for fundamental mode S-band multiple-beam amplifiers. *IEEE Trans. Plasma Sci.* **3**, 1212–1222 (2004).
17. Liang, H., Xue, Q., Ruan, C. & Feng, J. Integrated planar three-beam electron optics system for 220-GHz folded waveguide TWT. *IEEE Trans. Electron Devices* **1**, 270–276 (2018).
18. Yin, S., Zhang, Z., Peng, Z., Zheng, Q. & Wang, Y. A new impregnated dispenser cathode. *IEEE Trans. Electron Dev.* **12**, 4258–4262 (2013).
19. Langmuir, I. & Blodgett, K. B. Currents limited by space charge between coaxial cylinders. *Phys. Rev.* **4**, 347–351 (1923).
20. CST Corp., "CST PS Tutorial," Darmstadt, Germany, see http://www.cst-china.cn
21. User Manual CST Particle Studio SUITE. *CST Corp* (Darmstadt, Germany, 2012).

Acknowledgments

Author contributions

C.R. initiated and charged the research project. P.W. and H.Z. conducted the model design and CST simulations, Y.S. performed the numerical calculations, J.D., Y.D. and Z.Z. contributed to the discussions and manuscript revision.

Competing interests

The authors declare no competing interests.

Additional information

Correspondence and requests for materials should be addressed to C.R.

Reprints and permissions information is available at www.nature.com/reprints.

Publisher's note Springer Nature remains neutral with regard to jurisdictional claims in published maps and institutional affiliations.